Daytime variations of absorbing aerosols above clouds in the southeast Atlantic

Ian Chang and Sundar A. Christopher

Department of Atmospheric Science, The University of Alabama in Huntsville

UAHuntsville ATMOSPHERIC SCIENCE

AGU Fall Meeting 2016

THE UNIVERSITY OF ALABAMA IN HUNTSVILLE

A41D-0067 15 December 2016

1. Background

•Quantifying absorbing aerosols within and above clouds, including optical properties, radiative effects, and heating rates remains a challenge.

•Geostationary sensor such as the Spinning Enhanced Visible and Infrared Imager (SEVIRI) enable the assessment of the diurnal variation of aerosols above clouds in the SE Atlantic.

•Radiative transfer models (RTM) provide a theoretical framework for assessing radiative effects and enabling satellite remote sensing studies.

•The goal of this study is to retrieve and examine the diurnal variations of optical properties of aerosols above clouds that could not be performed from polar-orbiting sensors. This effort would provide a more accurate assessment of the radiative effects of aerosols and clouds.

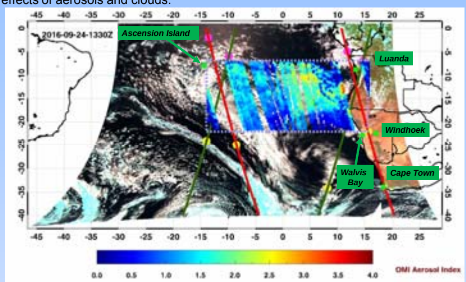

Figure 1. SEVIRI pseudo-color composite (Red=1.64 Green=0.81 Blue=0.64 on 24 September 2016 at 1330Z over the southeast Atlantic. Red and green transects represent the daytime and nighttime CALIOP overpasses, respectively. Overlay within the purple box is the OMI Above-cloud Aerosol Index (OMI data source: http://avdc.gsfc.nasa.gov/pub/data/satellite/Aura/OMI/V03/L2/OMACA/)

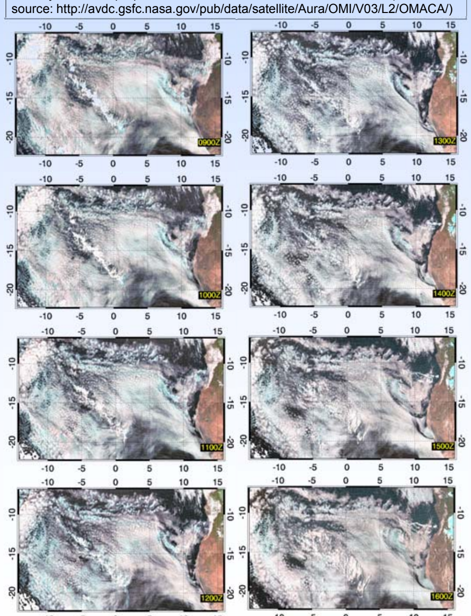

Figure 2. Pseudo-color composite showing the hourly variations of clouds between 09Z-16Z in the purple box from SEVIRI on 24 September 2016.

2. Data and Methods

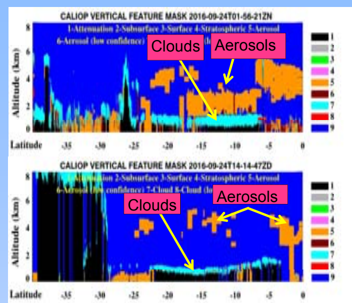

Figure 3. Daytime and nighttime CALIOP overpasses in the SE Atlantic on 24 September 2016.

Table 1 (right). The increase from 3 to 8 solar channels in METEOSAT Third Generation era will offer more accurate retrieval.

•Use the daytime (1330Z) CALIOP overpass and the most recent nighttime overpass (0130Z) from 12 hours ago in this region. Assume aerosol above cloud exists between latitudes bounded by the 2 overpasses.

•Simultaneously retrieve aerosol optical depth (AOD), cloud optical depth (COD), and cloud effective radius (CER) from look-up-table generated from DISORT using the spectral signatures and heterogeneity metric (5 by 5 σ/μ) from SEVIRI during daytime (9-15Z). Retrieval is done for pixels where both the solar and viewing zenith angles are < 65° Aerosol optical properties are based on SAFARI 2000 (Haywood et al. 2003, JGR) derived by Meyer et al. 2015 (JGR) (SSA_{550}= 0.91).

•Find the beginning and the end of aerosol clusters (10 consecutive pixels) along each swath.

•Retrieval is bounded within the daytime and nighttime overpasses (4 in 24 hours) and by the southernmost northbound and the northernmost south bound. No retrieval is done when the southernmost northbound is south of the northernmost southern bound.

MSG (current)	MTG (future)	GOES-R
	0.444 µm	0.47 µm
	0.510 µm	
0.635 µm	0.640 µm	0.64 µm
0.81 µm	0.865 µm	0.86 µm
	0.914 µm	
	1.380 µm	1.37 µm
1.64 µm	1.610 µm	1.6 µm
	2.250 µm	2.2 µm
3.9 µm	3.8 µm	3.9 µm
6.25 µm	6.3 µm	6.2 µm
		6.9 µm
7.35 µm	7.35 µm	7.3 µm
8.7 µm	8.7 µm	8.4 µm
9.66 µm	9.66 µm	9.6 µm
10.8 µm	10.5 µm	10.3 µm
		11.2 µm
12.3 µm	12.3 µm	12.3 µm
13.3 µm	13.3 µm	13.3 µm

3. Diurnal variations

Retrieval frequencies

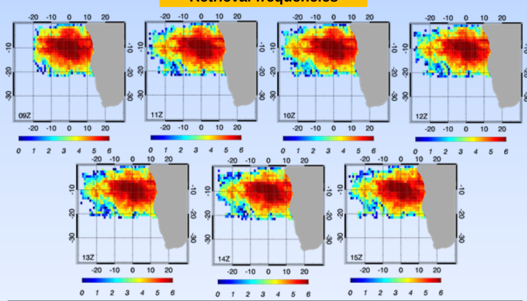

Figure 4 Mean hourly natural logarithm of AOD, COD, and CER retrieval frequencies within the CALIOP domain. Spectral signatures (solar and thermal channels) and heterogeneity metric (HM) are used for pixel filtering. The highest frequency occurs at locations where the closed-cell stratocumulus clouds are mostly occurred, which is slightly off the coast of the coastal regions.

Above-cloud aerosol optical depth

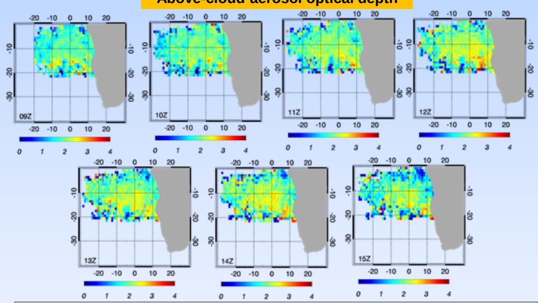

Figure 5. Mean hourly above-cloud AOD during the daytime (9-15Z) shows a fairly consistent pattern throughout the day and generally higher near the coastlines and south of 10°S. The limited spectral information results in biases and need comparison with other sensors.

Below-aerosol cloud optical depth

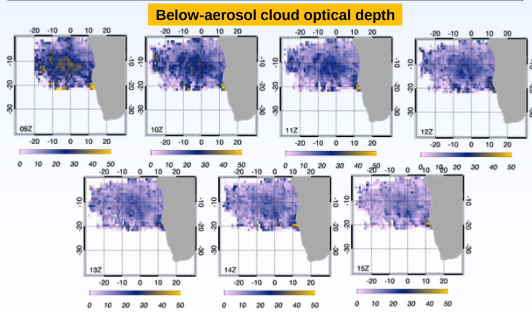

Figure 6. Mean hourly below-aerosol COD during the daytime (9-15Z) decreases throughout the day due to increased solar heating at cloud-top (i.e., decrease total radiative heating rates).

Below-aerosol cloud effective radius

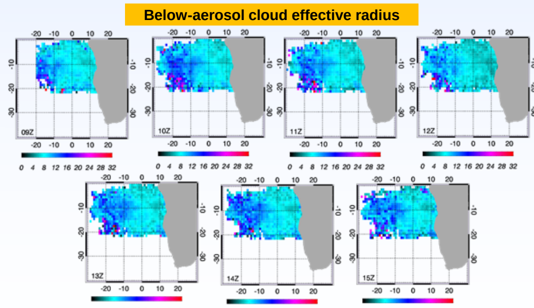

Figure 7. Mean hourly below-aerosol cloud effective radius (in micron) during the daytime (9-15Z) shows a fairly consistent values throughout the day. The cloud particle sizes generally increase westward due to decreased aerosol concentration.

4. Radiative fluxes and heating rates

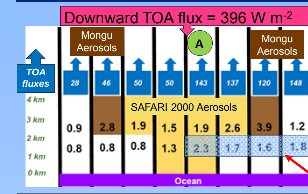

Model input parameters
Date: 1 September 2016
Position: 15°S 5°E
Aerosol optical depth = 0.6
Cloud optical depth = 9.0
Cloud effective radius = 12.8 µm

Figure 8. Diurnally-averaged fluxes and radiative heating rates on 1 September 2016 at 15°S 5°E for 8 aerosol and cloud scenarios. Optical properties (e.g., single scattering albedo) and vertical distributions of aerosols and clouds affect radiative fluxes and heating rates. Aerosols also enhance the heating rates in the cloud layer (more details in ***Chang and Christopher, QJRMS***).

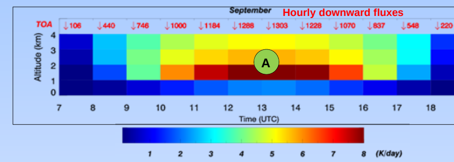

Figure 9. Monthly-averaged diurnal variations of radiative fluxes and radiative heating rates in September at 15°S 5°E. The aerosol and cloud vertical distributions are based on Scenario A in Figure 8. The largest vertical variation of heating rates occur at lowest solar zenith angle (i.e, highest downwelling flux). Further details are discussed in ***Chang and Christopher, QJRMS***).

5. Summary

• Daytime variation of above-cloud AOD and below-aerosol cloud effective radius are generally consistent throughout the day. The mean above-cloud AODs are generally ~1.8 and the mean CER is ~9.8 µm throughout the region. However, the limited spectral information from SEVIRI limits the retrieval capabilities compared to polar-orbiting sensors.

• The COD decreases during daytime as expected due to a decrease in total radiative heating rates (mainly in the shortwave heating rates). The mean COD decreases from 20 to 10 from 9Z to 15Z, reflecting the typical diurnal cloud cycle of stratocumulus clouds (e.g., Wood 2012, MWR).

• Vertical distributions of aerosols and their optical properties affect the direct radiative effect and the downwelling fluxes reaching cloud top.

6. Future investigations

•Expand the analysis to include southeast Atlantic and southern Africa with other retrieval techniques.

•Consolidate aerosol radiative effects that include aerosols above clouds, land, and ocean.

•Incorporate aerosol optical properties acquired from recent field experiments (e.g., ORACLES, LASIC, and CLARIFY etc.) to estimate the aerosol radiative effects.

•Inter-compare with polar-orbiting sensors and field experiment measurements.

•Trace the transport/trajectory of aerosols from the emission source region using geostationary sensor and then assess their optical/microphysical/radiative properties.

•The GOES-R series will offer unprecedented capabilities for studying the diurnal variations of aerosols and clouds over the Americas.

7. Recent publications

Chang, I. and S. A. Christopher (2016), The impact of seasonalities on the direct radiative effects and radiative heating rates of absorbing aerosols above clouds. Submitted to the *Quarterly Journal of the Royal Meteorological Society*.

Chang, I. and S. A. Christopher (2016), Identifying absorbing aerosols above clouds from the Spinning Enhanced Visible and Infrared Imager coupled with NASA A-Train multiple sensors, *IEEE Transactions on Geoscience and Remote Sensing*, **54**, 3163–3173.

Acknowledgement

This research is supported by the NASA Earth and Space Science Fellowship (NNX15AN29H) and NASA CALIPSO program.

E-Mail: **ian.chang@nsstc.uah.edu, sundar@nsstc.uah.edu**
http://www.nsstc.uah.edu/users/ian.chang/
http://www.nsstc.uah.edu/~sundar/index.html